Application of a microgrid with renewables for a water treatment plant

Soshinskaya, Mariya; Graus, Wina; van der Meer, Jos; Guerrero, Josep M.

Published in:
Applied Energy

DOI (link to publication from Publisher):
10.1016/j.apenergy.2014.07.097

Publication date:
2014

Document Version
Early version, also known as pre-print

Application of a microgrid with renewables for a water treatment plant

Mariya Soshinskaya[a,b], Wina H. J. Graus[a]*, Jos van der Meer[b], Josep M. Guerrero[c]

a Copernicus Institute of Sustainable Development, Utrecht University, The Netherlands
b Waternet, The Netherlands
c Microgrids Research Programme, www.microgrids.et.aau.dk
Department of Energy Technology, Aalborg University, Denmark, email joz@et.aau.dk

* Corresponding author
Wina Graus, Copernicus Institute of Sustainable Development, Utrecht University
Heidelberglaan 2, 3584 CS Utrecht The Netherlands
+ 31 30 253 1222, email: w.h.j.graus@uu.nl

Keywords
Microgrid; Renewable Energy; Drinking water plant; Distributed Generation; Energy Storage

Acronyms
Renewable Energy (RE), Distributed Generation (DG), Depth of Discharge (DOD), Demand Response (DR), Drink Water treatment Plant (DWP), Energy Storage System (ESS), Grid-Connected (GC), Net Present Value (NPV), Operation & Maintenance (O&M), Payback Period (PBP), Photovoltaic (PV), Stand-Alone (SA), Vanadium Redox Battery (VRB)

Abstract
This research explores the techno-economic potential for a predominantly renewable electricity-based microgrid serving an industrial-sized drink water plant in the Netherlands. Grid-connected and stand-alone microgrid scenarios were modelled, utilizing measured wind speed and solar irradiation data, real time manufacturer data for technology components, and a bottom-up approach to model a flexible demand from demand response. The modelled results show that **t**here is a very high potential for renewable electricity at the site, which can make this drink water treatment plant's electricity consumption between 70-96% self-sufficient with renewable electricity from solar PV and wind power production. The results show that wind production potential is very high onsite and can meet 82% of onsite demand without adding solar PV. However, PV production potential is also substantial and provides a more balanced supply which can supply electricity at times when wind production is insufficient. Due to the supplemental supply over different parts of the day, adding solar PV also increases the benefits gained from the demand response strategy. Therefore, a solar-wind system combination is recommended over a wind only system. A 100% renewable system would require extremely large battery storage, which is not currently cost effective. Ultimately, even at the low wholesale electricity and sell-back price for large electricity consumers, grid-connection and the ability to trade excess electricity is extremely important for the cost-effectiveness of a microgrid system.

1. Introduction

Due to the energy intensity of the industrial water treatment process and the high electricity costs associated with it, it is interesting to investigate whether water treatment plants can become decentralized microgrids to decrease dependence on (grey) power and rising electricity prices, yet still maintain water production using clean energy sources. A microgrid can be seen as a small scale electricity grid, which includes distributed generation and/or energy storage systems that supplies local consumption loads, being able to operate in both grid-connected and stand-alone islanded modes (Guerrero, 2013). While there are some examples of renewable energy (RE) based microgrids around the world that illustrate the benefits of producing and consuming renewable electricity onsite, there has been little research on the potential of a renewable-based hybrid system at a much larger scale and in a Dutch context where wind speeds are higher and solar irradiation more moderate. Thus, this research aims to identify the technical potential of integrating solar photovoltaic (PV) and wind power with demand response into a grid-connected versus stand-alone microgrid at a Dutch drink water treatment plant.

Self-sufficient energy systems already have been set up in a number of developing countries in order to help with the implementation of rural off-grid electrification in countries such as China, Mexico, Kenya and Bangladesh. The energy systems often consist of PV with battery packs or even backup diesel generators and are located in tropical regions (Urmee et al., 2009). However, these focus on a small rural energy demand, and therefore cannot be compared to the energy intensive power demand of an industrial process in a developed country. Multiple load microgrid examples also exist internationally, which meet the demand from residential and commercial buildings. For example, the Sendai microgrid in Japan has been able to supply five university buildings, an aged care facility, and a high school. The majority of this microgrid is comprised of reciprocating engines and supplemented with PV, a fuel cell, and battery storage. It is normally grid-connected to help deal with the intermittency of its renewable energy generation, although it is not allowed to feed power back to the grid, which is a common barrier for grid-connected microgrids (Irie, 2012). While this shows that larger load microgrid implementation is feasible, it does not indicate the feasibility of a predominantly RE-based microgrid at such a scale since most of these examples rely on conventional generators. In the context of the Netherlands, one such RE-based microgrid was tested in the village of Bronsbergen. The PV-battery microgrid with grid-connected and islanding capability was a test pilot, but was ultimately not economically viable due to the amount of storage required and the significant capital costs associated with the storage capacity (Cobben, 2008). As far as we know, no other Dutch microgrid examples have been documented.

There are also limited pilot cases and literature about the application of a microgrid to an industrial scale water treatment plant. In California there is an energy storage demonstration project implemented at a water treatment plant in 2006 in combination with a number of decentralized loads that could potentially be configured as a microgrid (Guerrero, 2010). Some literature discusses the feasibility of renewable energy powered water desalination plants and hybrid systems to show the sustainable application of renewable sources in water pumping systems (Lindemann, 2004; Mahmoudi et al., 2008; Ramos & Ramos, 2009). In the former, a seawater desalination plant in the Arabian Gulf is supplied by a stand-alone 750kW wind energy plant and a reverse osmosis (RO) plant was supplied by a stand-alone 4.8kWp PV system with additional battery storage of 60kWh[1]. However, these are

[1] Although desalination and reverse osmosis are different water treatment processes than ground water treatment, they are comparable in energy usage; with the latter potentially needing more energy in the future as new drinking water regulations will increase the use of higher energy consuming processes, such as ozone and membrane filtration (WateReuse, 2011)

small scale systems that do not incorporate the energy-intensive pumping of water to distribute it. Ramos & Ramos (2009), on the other hand, modelled stand alone and grid-connected hybrid energy systems of wind/PV/battery combinations on a water pumping system in Portugal and showed that wind and PV energy can complement each other to enhance system reliability; although systems with a greater proportion of PV were less cost-effective.
These studies are still smaller scale than an industrial sized water treatment plant and are targeted for areas with greater solar primary energy and lower wind speeds compared to the Netherlands. Additionally, these hybrid systems were simulated four or more years ago, when the capital costs, particularly for PV, were significantly higher than today.

In conclusion there is a knowledge gap when it comes to the technical and economic feasibility of a predominantly RE-based microgrid for a Dutch drink water treatment plant due to the novelty of smart grid technology, variety of microgrid structures, and incomparable internal, environmental, and regulatory conditions from other microgrid cases. This research aims to assess the application of a smart microgrid to a large scale industrial water treatment plant in the Dutch context. By taking a scenario approach of different combinations of DG, storage, DR, and grid-connection, it aims to identify the technical and economic feasibility of integrating DG at a drink water treatment plant into a microgrid to directly meet its demand with local supply.

2. Methodology

Due to the large amount of space required for the water treatment process and the distance from many residential homes, the drink water treatment plant (DWP) in Nieuwegein is a good candidate for wind and solar energy, located along the Lek Canal with 10,300 m^2 of roof surface area and about 70,000 m^2 of land on Parceel Zuid (Meer, 2012; Velden, 2011). Site description Heat demand at the site is relatively negligible, and in turn is not included. The lack of methane-producing biomass from the groundwater treatment process would require the plant to be dependent on purchasing large amounts of wood supply for biomass electricity generation to be a viable option. The sustainability of this option is questionable as this would require large amounts of land use elsewhere. Therefore, only wind and solar electricity potential are explored.
To model the proposed microgrid case HOMER modelling software is used to determine the fraction of onsite electricity demand that could be supplied by locally produced renewable electricity and whether that would create value for the system compared to the current base case of purchasing all electricity from the grid. There are a large number of different models available to investigate the integration of renewables. The HOMER (Hybrid Optimization Model for Electric Renewables) energy model, developed in 1992 by the National Renewable Energy Laboratory in the USA, is very suitable for this research (Connelly et al., 2010; COMMEND, 2012; HOMER Energy, 2013). Other model options include EnergyPlan or H2RES, but are not as useful in simulating microgrid energy systems because EnergyPlan is a deterministic model and does not optimize investment costs, and H2RES does not simulate grid-connection.

The first step of this research was defining the electricity load for an industrial water treatment plant (see section 2.1). Grid-supply was defined based on Waternet's contracted supply and electricity prices (see section 2.2). The potential for locally produced solar PV and wind power was then modelled based on the local geography and climate. The amount of renewable energy supply also has implications on the amount of storage, back up generation, storage, and/or demand response that will be necessary to balance the intermittency of the renewable and ensure a stable power supply (see section 2.3).

All of these microgrid components were then used as inputs in the HOMER model. Since microgrids can have different configurations based on the RE potential, technology sizing, and need for back up generation, and/or storage, a variety of scenarios with different electricity mixes and component capacities were run to see which one is the most cost-effective. Since grid-connection is also a way to regulate intermittency, all scenarios were run in grid-connected mode. Additionally, in order to gauge whether the drink water plant can be completely self-sufficient without depending on the grid, standalone scenarios were also run to test the technical and economic feasibility of this option.

2.1 Electricity Demand

In 2012, the DWP required 16.85 GWh of electricity to produce about 98 illion cubic meters of water, which is slightly higher than the 16 GWh average annual electricity demand over the years 2008-2012 (Waternet, 2013). In the coming years an annual electricity demand of 16.5-17 GWh is expected (Braam, 2013) and will be used in the model.

Unlike residential electricity demand, which follows an oscillating electricity distribution between the day and night, with more power used during the day and less at night, the distribution of power consumption for industrial drink water treatment over a day and a week is relatively flat and stable, with an average load of 1900 kW in 2012. Peak electricity was 3222 kW in July.

Pumping makes up 94% of the electricity demand at DWP, 13% of which is for the run-water pumps bringing water into the treatment process from the Lek Canal and 81% for the distribution pumps transporting pre-treated water to its direct customers and storage reservoirs (based on Waternet, 2012a, 2013a and 2013b). Demand response is useful in altering the level of the electricity consumption in response to the availability of wind and/or solar power for a period of time due to the large potential for integrating these renewable electricity sources onsite. In order to keep the treatment process stable, the electricity consumption of run-water pumps and the electricity demands of the internal buildings and processes are assumed to be inflexible. However, this still leaves a maximum flexible demand of 81% from the distribution pumps, which pump water more or less continuously throughout the day. Nevertheless, this flexibility is affected and limited by:

- customer demand,
- storage capacity (Leiduin Dunes),
- and pump and transport network characteristics

Table 1 breaks down the average hourly and annual required customer demand for the site, along with the annual power usage needed to distribute the annual water demand. These operating demands are more or less constant 24 hours in the day and every day of the week, with some ranging hourly demands from some clients taking in about 1000 m^3 per day less on the weekends (Braam, 2013). Thus, there is never a point in the day or week when immediate customers are not demanding water.

Table 1. Summary of average hourly and annual customer demand

	Production		kWh Required*
CUSTOMERS	Avg. Hourly Demand (m^3/hr)	Avg. Annual Demand (million m^3/yr)	Avg. Annual Electricity Required (million kWh/yr)
Total excl Dunes	7468	43.21	6.04
Total incl Dunes	13,768	98.21	13.73
Total incl Min Dunes	9600	61.89	8.65

*based on 0.14 kWh/m^3 power consumption of distribution pumps for total water production in 2012 (Waternet, 2013c)

The Leiduin Dunes take in 50-55% of average water production (Stouten & Pinksteren, 2010). Unlike the customers who use the water immediately for their operations, the Leiduin Dunes are more of an intermediary receiver, since they are used to naturally filter the pre-treated water from the DWP for about 3 months before the water treatment plant in Leiduin[2] finalizes the process (Heck, 2013).

In order to consistently meet the required customer demands, the electricity usage required to meet those demands is considered inflexible and thus included in the inflexible primary load. The Dunes, on the other hand, have the flexibility of accepting water intake between 0 – 10,000 m^3/hour (Braam, 2013). However, in order to maintain a certain level of pressure and consistency in water flow to the dunes, it is assumed that about 2000 m^3/hour is fixed since this is the amount produced by the 4 lowest rated pumps which will be running anyway to meet the other customer demands. Running at the lowest pumps is not uncommon, particularly in the winter months when customer demand is low.

By taking into consideration the customer water demands and the water storage buffer capacity at the Dunes and onsite pump installations, 29% of normal 16.7 GWh annual demand is calculated and modelled to be flexible with an additional 15% of flexibility to pump more water to the Leiduin Dunes, which have an approximate 18 million cubic meters water storage buffer above normal water demand (55 million m^3).

In order to integrate loads and DG with demand response and load management in a microgrid, specific microgrid hardware and Information Technology (IT) controls are necessary to facilitate communication and control between electricity demand and supply. There is a lot of research and development on different forms of hardware and controls for microgrids, with demonstration and pilot cases popping up around the world, as mentioned in the problem definition. However, this hardware and IT systems have not yet reached full commercialization so their costs are case specific and difficult to estimate. This research assumes microgrid hardware/IT fixed capital costs of about €96,000 ($129k at 0.748 average 2011 exchange rate) based on a Canadian case study done by Morris et al. (2011) to create a framework for the cost benefit analysis of microgrids. This includes all controllers, communications devices, and disconnect switches and assumes that the microgrid infrastructure distribution feeders already exist.

2.2 Electricity Supply

Since the DWP site has a load connection of 3 phase of 300A, this allows it to pay wholesale electricity prices, rather than retail prices, as a bulk consumer (Braam, 2013). The DWP pays 0.06975 €/kWh off-peak and 0.08847 €/kWh during peak hours if it doesn't produce and consume electricity on-site in 2013. For an electricity consumption of

[2] The power consumption for this final treatment process is not included in this research since the Leiduin water treatment plant is not a direct neighbor of the DWP and therefore cannot be directly connected to the onsite microgrid.

16.8 GWh in 2013, DWP pays about €1.4 million, with a fixed interconnection cost of about €110k included (Knibbe, 2013).

In the Netherlands small consumers are treated differently than large consumers, where the former receives standard sell back rates from their energy supplier and the latter has case by case contracts. Since DWP is a large consumer, it has an agreement with the energy supplier that the sell back rate for any renewable energy production is equal to the commodity price (Knibbe, 2013). Therefore, selling back to the grid has no advantage over using the electricity directly onsite.

Wind Power

The site-specific potential for wind energy depends on the wind speeds at the location. Figure 1 illustrates the measured average wind speeds in the Netherlands at 10m (left) and computed average wind speeds at 100m (right). Locations with average annual wind speeds of more than 5.6 m/s are suited for wind production (Manwell et al., 2009). At 52.029559^0 latitude, 5.112426^0 longitude, the DWP is located Northwest of Cabauw and Southwest of De Bilt, putting it in the 4-4.5 m/s wind speed category at a height of 10 m and 6.0-7.0 m/s wind speed category at 100m, according to Figure 1. Due to its close proximity to Cabauw (15km) and similar wind speed category, 2012 measured wind speed data from the Cabauw wind station is used to simulate the wind climate at the DWP. Average monthly wind speed at 10m height measured in 2012 can be seen in Figure 2, with an average annual wind speed of 4.47 m/s. Analyzing measured hourly KNMI data from 2002-2011, average wind speeds ranged from 4.16 m/s to 4.69 m/s, with the 10 year average at 4.49 m/s. Therefore, 2012 measured hourly data from Cabauw is a good representative data set to model from.

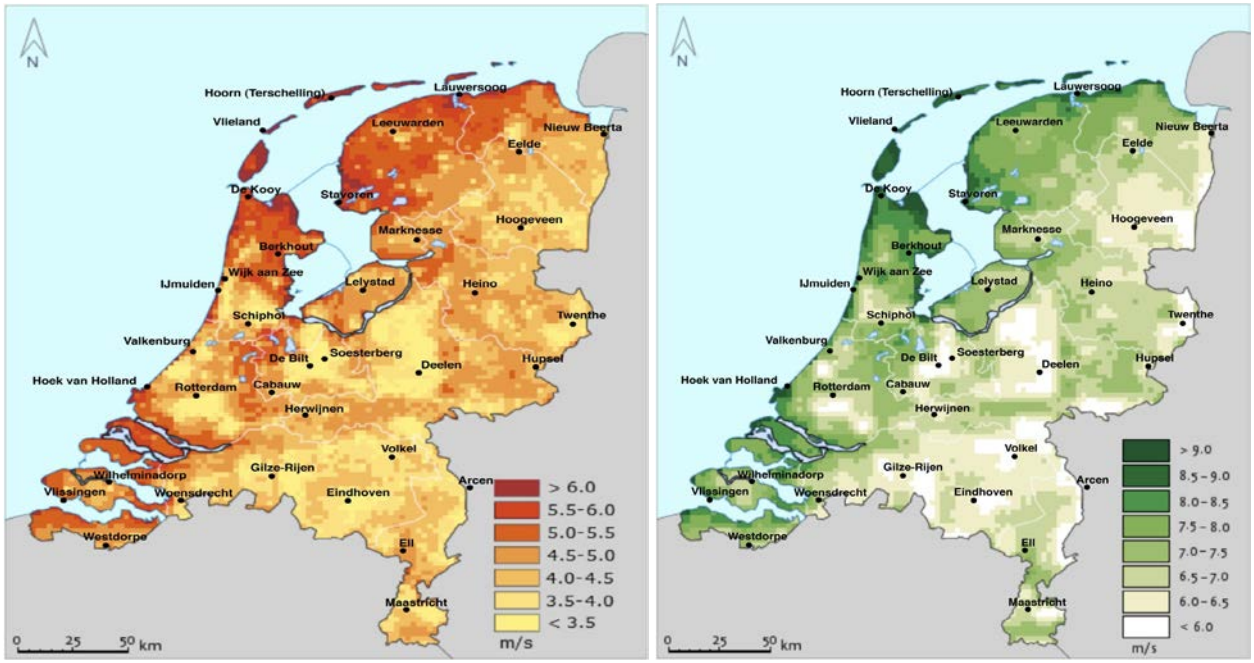

Figure 1. Average annual wind speeds in the Netherlands, (left at 10m; right at 100m) (KNMI, 2012)

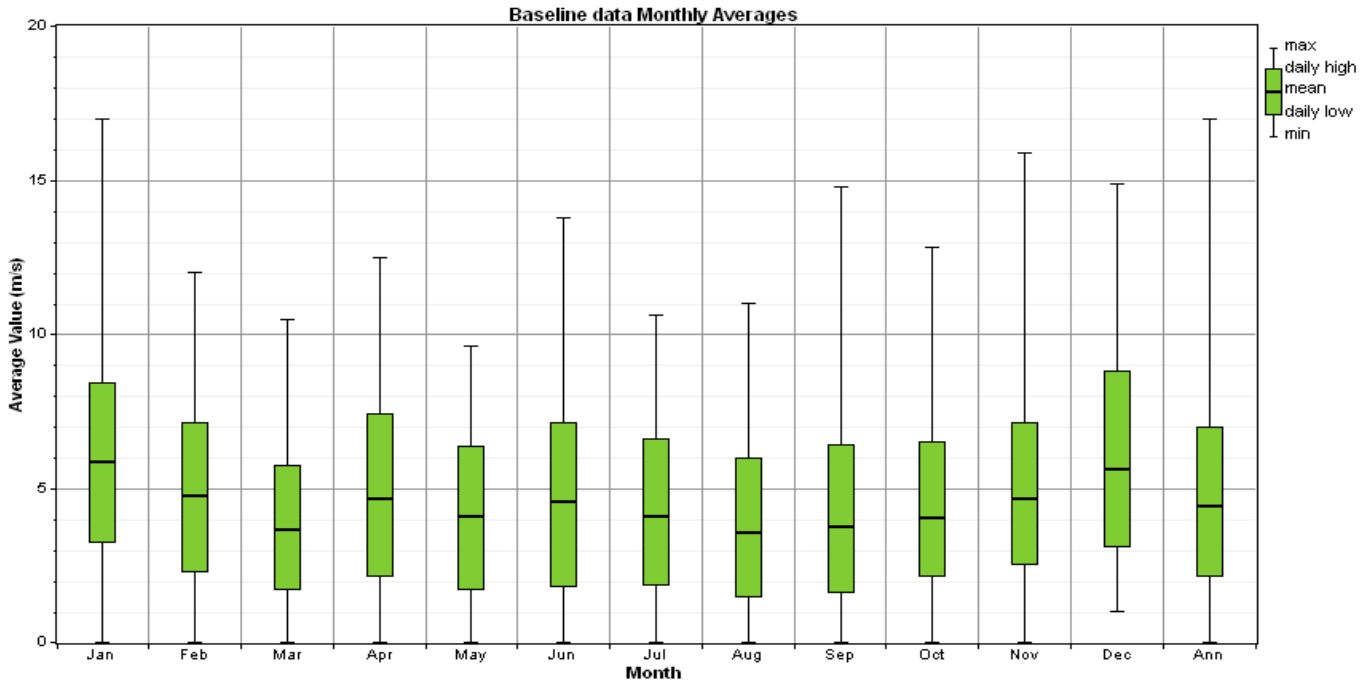

Figure 2. 2012 wind speed monthly averages in Cabauw at a height of 10m (KNMI, 2012)

The most commonly used type of wind turbine is a horizontal axis turbine with a three blade rotor spinning in a vertical plane attached to a nacelle. The Vestas V90 – 2.0 MW wind turbine is an example and is specially designed for low to medium wind speeds, such as those found at the DWP. Therefore, it will be used in this research.
Since the KNMI data is measured at a height of 10m, the following formula is used to adjust the wind speed at 105m, the hub height of the selected turbine, and a 0.03 surface roughness length at the 10m (Andrews & Jelley, 2007):

$$\frac{U_{hub}}{U_{anem}} = \frac{\ln(z_{hub}/z_0)}{\ln(z_{anem}/z_0)}$$

Where:

U_{hub} = the wind speed at the hub height of the wind turbine [m/s]
U_{anem} = the wind speed at anemometer height [m/s]
z_{hub} = the hub height of the wind turbine [105m]
z_{anem} = the anemometer height [10m]
z_0 = the surface roughness length [0.03m]
ln*(..)* = the natural logarithm

Adjusting the wind speeds at 105m leads to an average wind speed of 6.25 m/s. This is in line with the 6.5 m/s (+/- 0.7) wind speed estimated in the wind potential study done by Ritzen & Gastel (2012), which used a weighted average of wind speed data sets from Schipol and Herwijnen, based on the distance from the DWP to the measuring stations.

Power output is calculated at standard temperature and pressure based on the turbine production curve in Figure 3 and the computed wind speeds from step 1. Additionally, an air density correction is applied since air is denser at

sea level than it is at a higher altitude and will therefore carry and transfer more energy to the blades of a wind turbine than air moving at the same speed at a higher altitude. The DWP is 1m above sea level, and therefore has relatively dense air, which improves power production. The following air density correction formula is used (Lambert, 2007):

$$P_{WTG} = (\rho / \rho_0)\ x\ P_{WTG,STP}$$

Where:

P_{WTG} = the wind turbine power output [kW]

$P_{WTG,STP}$ = the wind turbine power output at standard temperature and pressure [kW]

ρ = the actual air density calculated based on altitude of site (1m at DWP) [kg/m^3]

ρ_0 = the air density at standard temperature and pressure (1.225 kg/m^3)

Source: Lambert, 2007

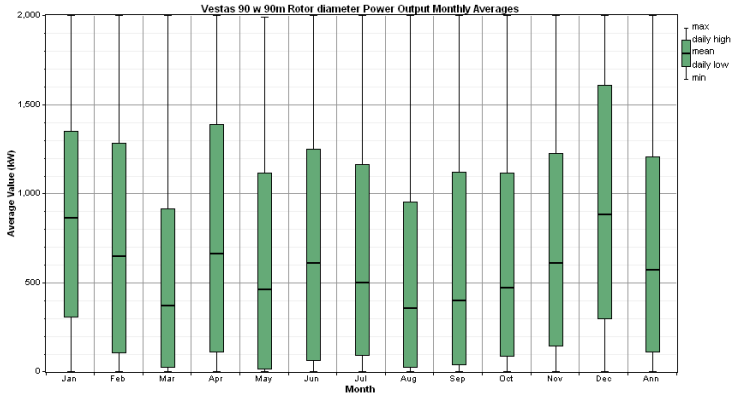

Figure 3. (Left) Reconstructed power curve for Vestas V90 2MW wind turbine (Vestas, 2012)

Figure 4. (Right) Simulated annual power output (kW) of 1 Vestas V90 turbine

This results in 5 GWh of annual electricity produced per turbine and a capacity factor of 28.6%, which is in line with the production results from Ritzen & Gastel (2012). Figure 4 illustrates that the higher wind speeds during the winter months lead to greater production compared to summer months. This is emphasized in Figure 5, which indicates that the average hourly winter output of a Vestas V90 wind turbine is 726 kW, 40.3% greater than the average summer power output of 433 kW per hour. There is also a stark difference in output from the daytime (here defined as 7am-7pm) versus night-time (7pm-7am). The largest difference between night and daytime power output is 64.7% during the summer months and the lowest day/night difference is 23% in the fall and winter. On a full year basis, the average output during the day is 39.4% higher than during the night.

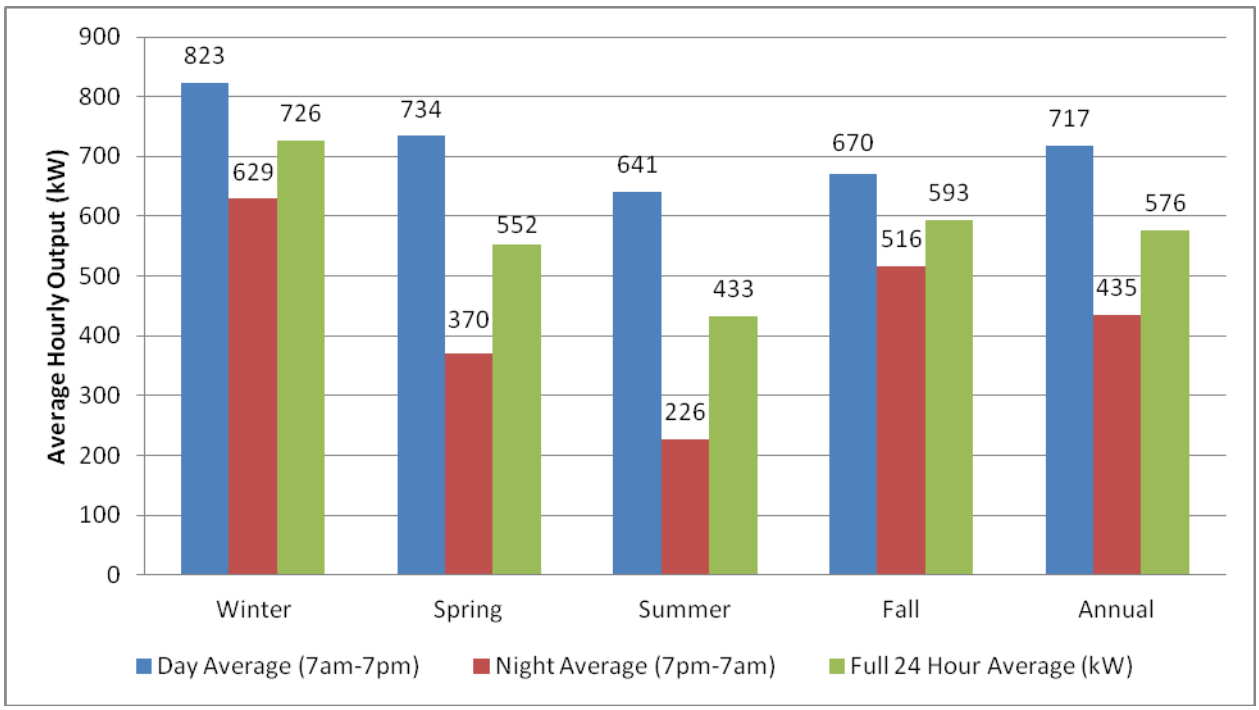

Figure 5. Average hourly output (kW) of 1 Vestas V90 on a seasonal, daily, and nightly basis

The total onsite potential for wind depends on the space requirement per turbine and space available onsite. The amount of space required for a wind turbine depends primarily on the height and diameter of the turbine both in relation to other turbines and the built environment. Normally a spacing of about 5 to 10 rotor diameters between turbines is necessary in order to maintain optimal wind speeds and production for each turbine (Andrews & Jelley, 2007). Taking into account the distance to nearby houses, shadow cast by the turbines, and noise effects on the surrounding environment Ritzen & Gastel (2012) suggest placing 3 turbines along the Lek Canal. However, assuming a 4 or 5 diameter spacing between turbines there is the potential for a fourth wind turbine to be placed about 400-500m south near Parceel Zuid. This would extend the shadow cast over Parceel Zuid, which could negatively affect the solar electricity potential if PV systems are placed there. Placing four V90 wind turbines at the DWP site along the Lek Canal results gives a maximum potential of about 20 GWh of wind electricity production per year. Thus, 0 to 4 turbines will be considered in the microgrid system configurations modelled in HOMER.

Average investment costs in Europe for a 2MW turbine in 2006 in Europe were about €1.2 million per MW (Wind Energy, 2009). Since this is a developed technology, costs have not drastically changed since then. The study done by Ritzen & Gastel (2012) for this specific site actually estimated total capital expense of about €1.4 million per MW, which is slightly higher than the EU average, but includes €218k in site-specific development costs. Table 2 below summarizes the cost assumptions used in modelling the wind turbine economics.

Table 2. Summary of cost figures used in economic simulation of chosen wind turbines

Lifetime	20 years
Initial Investment Costs	€ 2,855,000 per turbine
Replacement Costs (at end of lifetime)[a]	€ 2,135,540 per turbine
Annual O&M (2% of initial investment)[b]	€ 57,000

[a] Based on a forecasted and conservative 20% capital cost reduction by 2030 and excluding the costs for replacing the foundation, which are about 6.5% of initial investment costs (Lantz et al., 2012; Wind Energy, 2009; WWI, 2012)

[b] For modern wind turbines the estimated annual operation and maintenance (O&M) costs are in the range of 1.5% to 2% of the original investment per annum (excluding development costs) (WWI, 2012).

Photovoltaic (PV) Power

Besides the solar irradiance, the total amount of electricity produced by solar PV heavily depends on the specific characteristics of the PV cells, like the conversion efficiency, the placement of the PV panels in relation to the sun, and de-rating factors which cause the PV cells to perform below the rated efficiency. Haberlin (2012) also indicates that ambient temperature affects power output; however, since HOMER does not explicitly model this effect, it is built into the de-rating factor (Lamberts, 2007). These will be discussed here as inputs into the model in order to calculate the total electricity potential for solar PV at the DWP.

The Netherlands receives about 1000 kWh/m^2/year (Haberlin, 2012). Figure 6 illustrates that more western regions of the Netherlands receive a higher solar irradiance than those Northeast. The DWP site is located in the center region, receiving about 365-370 kJ/cm^2, which is the same as Cabauw. Therefore, KNMI measured data for Cabauw is used again. However, since solar irradiance data is only measured as a daily average instead of on an hour to hour basis, this full year data is incompatible with the HOMER model since it can model either hourly (or less) time steps, or interpolate monthly averages. Therefore, monthly averages of solar irradiance of the past decade (2003-2012) were calculated from measured data for Cabauw, see figure 7.

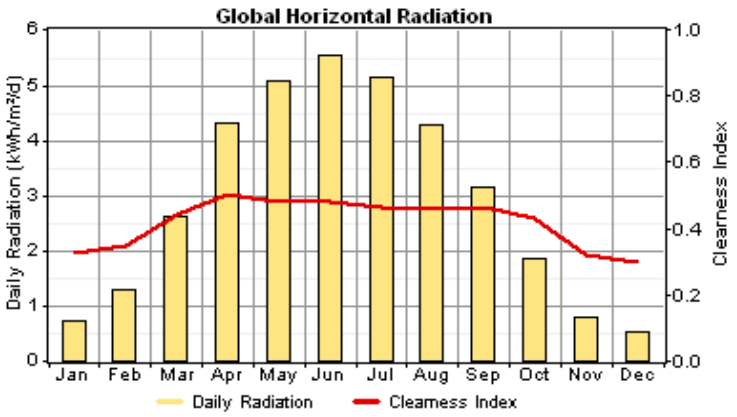

Figure 6. (Left) Solar irradiance in the Netherlands (KNMI, 2012)

Figure 7. (Right) Average solar radiation and clearness index at DWP Nieuwegein based on 2003-2012 measured average daily solar irradiance in Cabauw , at 52° 1' N latitude and 5° 6'E longitude.

At current levels, PV technology used for commercial purposes ranges from 12-16% in conversion efficiency, which differs depending on cell type and manufacturer. The PV module chosen for this research is the monocrystalline silicon cell CSUN255-60M model from ChinaSunergy, which is a proven cost-effective technology. The efficiency of a module is 15.71% at standard testing conditions (STC) [T = 25° C, 1000 W/m^2] and yields about 157 W_p /m^2 (refer

to Table 3 for a summary of characteristics of the modeled PV cells). However, this efficiency is slightly less at nominal operating cell temperature (NOCT) [T= 20° C, 800 W/m^2], which is modeled by taking into account the NOCT cell temperature. The temperature coefficient of power, which is -0.43%/°C for the chosen PV module, indicates how strongly the PV array power output depends on the cell temperature, meaning the surface temperature of the PV array which is influenced by the ambient temperature. Since power output decreases with increasing cell temperature (Lambert, 2007), KNMI average monthly ambient temperature data from 2001-2012 is used in the model to calculate the cell temperature at each step using the following equation, in accordance with Duffie and Beckman (1991)

$$T_c = \frac{T_a + \left(T_{c,NOCT} - T_{a,NOCT}\right)\left(\frac{G_T}{G_{T,NOCT}}\right)\left[1 - \frac{\eta_{mp,STC}\left(1 - \alpha_p T_{c,STC}\right)}{\tau\alpha}\right]}{1 + \left(T_{c,NOCT} - T_{a,NOCT}\right)\left(\frac{G_T}{G_{T,NOCT}}\right)\left(\frac{\alpha_p \eta_{mp,STC}}{\tau\alpha}\right)}$$

Where:

T_c = the PV cell temperature [°C]
T_a = the ambient temperature [°C]
$T_{c,NOCT}$ = the nominal operating cell temperature [°C]
$T_{a,NOCT}$ = the ambient temperature at which the NOCT is defined [20°C]
$G_{T,NOCT}$ = the solar radiation at which the NOCT is defined [0.8 kW/m^2]
G_T = the solar radiation striking the PV array [kW/m^2]
α_p = the temperature coefficient of power [0.43%/°C]
$\eta_{mp,STC}$ = the electrical conversion efficiency of the PV array at maximum power [%]
$T_{c,STC}$ = is the cell temperature under standard test conditions [25°C]
$\tau\alpha$ = the solar transmittance of any cover over the PV array *the solar absorptance of the PV array [0.9]

Table 3. Summary of characteristics of modelled PV modules (Lambrechts, 2012; CSUN, 2012)

CSUN255-60M	Dimensions
Length	1640 mm
Width	990 mm
Height	40 mm
Surface area of 1 module	1.62 m^2
	STC 1000W/m^2
Maximum power (P_{max})	255 W_p
Open circuit voltage (U_{oc})	38.0 V
Short circuit current (I_{sc})	8.82 A
Optimum operating voltage (U_{mpp})	30.7 V
Optimum operating current (I_{mpp})	8.3 A
Module Efficiency (η_{module})	15.71%
Max production per m2	157 W_p
Lifetime	25 years
Nominal cell temperature	45°
Temperature coefficient of power	-0.43% / °C

Power output of the PV panels is also highly dependent on how and where the PV modules are placed, since the following variables influence electricity yield: tilt angle of the array, azimuth, ground Reflectance and de-rating factors.

In order to maximize electricity production, the default tilted angle should be equal to the location's latitude plus 15 degree in winter or minus 15 degrees in summer. At 52° latitude at the DWP site, this would be 77° in the winter and 37° in the summer. However, the sun's path and solar altitude vary throughout the year and from year to year. Thus a tilt angle of 28° – 30° is recommended to optimize the capture of solar radiation; however, tilt angles between 20° – 60° are possible without significant losses in yield (Renewable Energy Concepts, 2012). This research will model with a slope of 29°. Tracking systems are available on the market to rotate the PV panels in accordance with the changes in the sun's orientation to maintain maximum optimum angles over time; however, these systems are less resistant to climatic conditions and require more maintenance (Lambrechts, 2012). Therefore, these are not considered for this research work.

The azimuth is the direction towards which the PV panels face. With fixed-azimuth systems, the panels are almost always oriented towards the equator, which is 0° azimuth in Europe because this ensures the highest yield. Therefore, the PV modules modeled in this research are geographically oriented south.

The ground reflectance is the fraction of solar radiation incident on the ground that is reflected back onto the PV array. Ground reflectance positively influences power output, with higher values having a more significant impact (ie. Snow-covered areas may have a reflectance as high as 70%). The site is a grass-covered area, which has a normal ground reflectance of 20% (Budikova et al., 2012). This value is used in calculating the radiation incident on the tilted PV panels, but it has only a modest effect (Lambert, 2007).

De-rating factors negatively influence the power performance of PV modules. Their performance is very sensitive to factors that may prevent the cells from capturing the sun's rays like dirt, snow cover, or shading from surrounding trees, buildings, etc. These factors can also be internal like wiring losses and aging PV cells. For example, the CSUN255-60M modules used have a power warranty of 90% at 10 years and 80% after 25 years (Lambrechts, 2012). Since HOMER does not separately include these in the model, a de-rating scaling factor is applied to the PV array power output to account for reduced output in real-world operating conditions compared to operating conditions at which the array was rated. Lambert (2007) suggests a normal de-rating factor between 80-90%. However, the PV pilot in Leiduin that used these PV modules had a simulated performance ratio of 82.7%, which includes the negative effects of linear shading on the module and the positive effects of ambient temperature on PV array performance (Lambrechts, 2012). The average temperatures in Nieuwegein are comparable to Leiduin. In order to account for the 90% power warranty after 10 years and any un-cleaned dirt or snow covering the panels over time, this simulated performance ratio is corrected by 90% to a comprehensive de-rating factor of about 75%.

The following equation is used in HOMER to calculate the output of the PV array (Lambert, 2007):

$$P_{PV} = Y_{PV} f_{PV} (G_T / G_{T,STC}) [1 + \alpha_p (T_c - T_{c,STC})]$$

Where:

- Y_{PV} = the rated capacity of the PV array, meaning its power output under standard test conditions [kW]
- f_{PV} = the PV derating factor [%]
- G_T = the solar radiation incident on the PV array in the current time step, which depends on the tilted angle (slope) of the PV panel and the ground reflectance (albedo) [kW/m^2]
- $G_{T,STC}$ = the incident radiation at standard test conditions [1 kW/m^2]
- α_p = the temperature coefficient of power [0.43 %/°C]
- T_c = the PV cell temperature in the current time step [°C]
- $T_{c,STC}$ = the PV cell temperature under standard test conditions [25 °C]

Since PV technology produces DC electricity, inverters are required to convert the DC power to AC power in order to be used by the system and injected into the grid. Since it has proven compatibility with the chosen PV modules based on the Leiduin PV pilot, the modeled inverter is the Sungrow SG30KTL inverter[3]. The maximum AC power output is 98.8% and inverter efficiency is 97.8% at full load, which is well above the required 95%. Normal inverter lifetimes are 15 years, so this will be assumed in this research.

Although at general measurement there seems to be about 7 hectares of ground space available on Parceel Zuid and about 1 hectare of roof space, these are not all suitable for placement of solar PV panels (Velden, 2011, Meer, 2012). Taking into consideration that PV cells perform better when more of them are contiguously connected, a surface area that allows for one large PV system is optimal. Therefore, only Parceel Zuid is considered. Not including the space rented to the nearby KWR research lab and for dogwalkers/horse grazing, the total area available for PV modules is about 3.6 hectares, i.e. 36,000 m^2 (Velden, 2011).

At 157 Wp/m^2 this PV technology requires about 6.37 m^2, or about 4 PV modules, to produce 1 kWp so that the maximum solar PV potential is 5,652 kWp. Depending on how many panels there are and how they are arranged, the space requirement is often adjusted by a factor of 2 to 6 depending on the location, in order to avoid panels from casting shade on each other (Haberlin, 2012). No literature states which factor to use specifically for the Netherlands, and PV system placement is very case specific. However, a factor of 2 was used for the Dutch pilot system in Leiduin so this will also be taken into account in this research (Meer, 2013). If adjusted by a factor of 2 the PV production potential is about 2,826 kWp, and if adjusted by a factor of 4 the PV capacity is 1,413 kWp. In order to see the effects of larger and smaller PV systems, the solar PV system sizes considered are: 0, 1.4 MWp, 2.8 MWp, and 5.6 MWp.

Table 4. Summary of cost assumptions for PV modules and inverter technology

PV System Cost Assumptions	PV modules	Inverter	Total PV System
Lifetime	25 years	15 years	
Initial Investment Costs	€ 820 / kW	€ 150 / kW	€ 952/ kW*
Replacement Costs	€ 400 / kW	€ 100 / kW	
Annual O&M	€ 4 / kW	Included in PV module	

*PV array to inverter ratios is assumed to be 1.13 (Lambrechts, 2012)

2.3 Storage and back-up generation

Electricity storage applications can be generally divided into power applications and energy applications. Power applications require high power output in relatively short period of time (seconds to minutes), in order to fulfill power quality and bridging power functions like ancillary services, voltage support, and assuring continuity of service when switching between generation sources. Energy applications, on the other hand, require storage of relatively large amounts of electricity for discharge durations of many minutes to hours, to fulfill energy management functions which decouple the timing of electricity generation and consumption by shifting energy use to a different point in the day when there is either more demand or grid prices are higher.

[3] Sungrow is the first and largest Chinese PV inverter manufacturer, founded in 1997, and as of today they have more than 400 MW of inverters installed in Europe (Sungrow, 2013)

Since a microgrid case optimally requires both power and energy applications, the practically and economically suitable technology options for this research are flow batteries, NaS (Sodium Sulfur) batteries, Ni-Cd (Nickel-Cadmium), and Electrochemical Capacitors. Flow batteries and NaS batteries are the only ones with much longer discharge times, which is important when intermittent renewable generation is not meeting demand. However, NaS batteries have high production costs and safety risks due to their extremely high operating temperature requirement, so flow batteries are the best option for this case. Moreover, flow batteries have a wider range of possible system rated capacities, which is important in this case research in order to properly size the storage system to the optimal energy generation mix (ESA, 2011).

HOMER models a battery based on its round-trip efficiency (energy discharged versus energy in), and lifetime (based on number of discharge/charge cycles the battery can withstand at a given DOD). Table 5 below summarizes the input specific parameters for a flow battery.

Table 5. Summary of VRB ESS Flow Battery Characteristics (Prudent Energy, 2012)

Roundtrip Efficiency	**80 %**
Cell stack lifetime	**15 years**
Electrolyte lifetime	**125 years**

Although flow battery technology is not yet a completely mature technology, its costs are still relatively lower than other technologies. However costs range significantly based on the size and design of the system. Based on 2007 estimates, initial investment costs can range from €750-2,750/kW for the cell stack and €200/kWh for the electrolyte energy storage, depending on the scale of the system and the amount of required electrolyte. These prices are expected to decrease to a lower level of approximately €500/kW and €100/kW as soon these systems are mass-produced on the market (Boer and Raadschelders, 2007). Table 6 summarizes the cost assumptions used in HOMER.

Table 6. Summary of storage cost assumptions[4] for VRB ESS Storage Systems (Prudent Energy, 2012)

	Cell Stack & Electrolyte Storage
Initial Investment	€577 / kW & €154 / kWh
Replacement	€385/kW
Variable O&M	€0.006/kWh

By integrating solar PV and wind power into the DWP microgrid system, the amount of power required from the grid can be significantly reduced. However, since solar and wind resources are both inherently intermittent in nature, the system design requires some form of backup generation, particularly if grid connection is interrupted for any reason, and especially if it needs to be in island (stand-alone) mode for a longer period of time. During grid-connection, back-up generators serve the purpose of meeting minimum demand if there is a short interruption in the grid since the grid normally provides the balance between generation and local demand onsite. However, in stand-alone systems, back-up generators can play a more significant role to help balance demand and supply locally.

In this case, the site already has two 660 kW diesel generator sets for back-up power production in order to maintain the water treatment and pumping process. Already having backup generators is not exceptional in this

[4] Based on low range estimates from www.pdenergy.com and converted to euros from dollars using a €1.3 Euro per USD conversion as of April 22, 2013.

case since constant water demand is imperative, so most industrial water treatment plants have backup generators already onsite for emergencies. Therefore, these onsite diesel generators will also be used in this research. Each set consists of a Cummins KTA 38-G3 engine and an AVK 0SG74M-4 Generator. These diesel generators are known for their reliability, and have been proven to be suitable for utility peaking plants, distributed generation facilities, peak shaving, and power management at commercial and industrial sites. Since these generators do not run all the time, their lifetime is expressed in hours. In this case, these generators have a lifetime of about 15,000 hours and 30% minimum load ratio, which is the minimum allowable load on the generator, as a percentage of it rated capacity (Cummins, 2012).

Table 7 summarizes the fuel consumption assumptions used for the modelled diesel generators and Figure 8 illustrates the fuel efficiency based on these fuel consumption assumptions. This fuel consumption pattern leads to a 0.01614 L/hr/kW rated Intercept coefficient, which indicates the no-load fuel consumption of the generator divided by its rated capacity.

Table 7. Fuel consumption assumptions for 600kW diesel generator (Diesel Service & Supply, 2013)

kW	Fuel Consumption (l/hr)
150	50.0
300	83.3
450	119.2
600	162.0

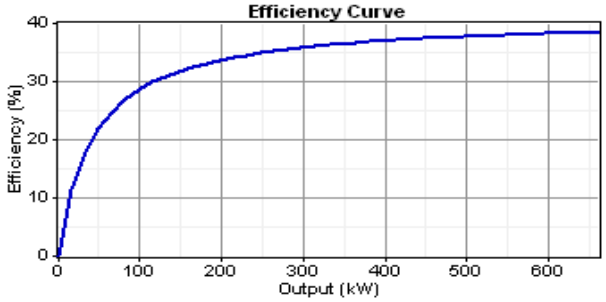

Figure 8. (Right) reproduced fuel efficiency curve based on fuel consumption data from Table 7

The initial investment for a 600 kW diesel generator runs at about $85,000, or about €65,000 euro using a 1.3 conversion (GeneratorJoe, 2013). However, since diesel generators already exist at the DWP site, these investment costs have already been incurred and are not relevant. However, at the end of their lifetime, which depends on how often they are used, they will need to be replaced. Assuming the diesel generators are a mature technology, prices will not decrease significantly over their lifetime so replacement costs are assumed to be 90% of the today's investment costs, although their lifetime in years depends on how often they are used. Table 8 summarizes the cost and fuel price assumptions used to model these back up diesel generators.

Table 8. Diesel generator cost & fuel price assumptions for each generator

Category	Amount
Initial Investment	€0
Replacement (90% of current prices)	€ 58,500
O&M	€ 8.58 /hr[a]
Diesel Fuel Price	€1.478/liter[5]

[a]O&M based on €0.013/kW cost for a generator running about 200 hours or less per year in study done in 2003 comparing costs of utility distributed generators in 24 case studies (EPRI, 2003). Although these are privately owned diesel generators, they are still quite large and more comparable to utility scale DG versus small scale DG.

[5] Diesel price as of April 16, 2013 (http://www.fuel-prices-europe.info/)

When there is a primary load and a flexible load, or deferrable load, the latter is second in priority behind the primary. However, the flexible load takes priority over charging the batteries. In order to consume any excess produced electricity, a load following strategy is employed so that the deferrable load is served only under these circumstances (or when the storage capacity reaches its limit). Storage and generators can be dispatched using two different strategies in HOMER: cycle charging or load following. Since this system has a high potential for wind and solar power, the load following dispatch strategy is used so that the deferrable load is only met when there is excess renewable electricity production. Since VRB battery storage has not reached full market maturity, and remains relatively expensive, it is expected that minimal storage will be needed in a grid-connected microgrid. However, in island mode when the microgrid is disconnected from the grid, battery storage will become more important in order to balance supply with demand.

2.4 Summary of Assumptions

Once the system components are modelled, HOMER runs 1 year cost-optimization simulations of the different combinations of system design and then ranks them based on net present cost. Table 9 summarizes the component system inputs based on the feasibility and needs of the DWP. HOMER filters out any infeasible combinations from the list of optimized systems.

Table 9. Summary of component sizing inputs

Technologies	Input parameters
Wind Production (nr of 2 MW turbines)	**0; 1; 2; 3; 4**
Solar Production (kW)	0; 1413; 2826; 5652
Converter (kW)	0; 1260; 2490; 5160
Flow Battery Cell Stack (kW)	0; 1000; 2000; 3000
Flow Battery Electrolyte Storage Tank (kWh)	0; 20000; 45000; 60000
Diesel Generators	0; 2x660Kw

Due to the multiple sizing options explored for each system component and the cases with and without demand response or grid connection, there are thousands of possible system designs. Therefore, the realizable and relevant system designs are chosen based on maximum renewable production possibilities, cost optimization, and for the sake of comparison. These scenarios are evaluated and compared based on technical and economic indicators, which are summarized in Table 10. Economic potentials are based on a 25 year project lifetime.

Table 10. Summary of technical and economic indicators used to evaluate and compare scenarios

Technical	Economic
Annual RE Production (GWh/year)	Levelized Cost of Electricity (COE) [a] (€/kWh)
Annual Generator Supply (GWh/year)	NPV[b] (€ million)
RE Fraction of Load (%)	Discounted PBP (years)
Annual Grid Purchases (GWh/year)	
Annual Storage Throughput (GWh/year)	

[a] Levelized Cost of Electricity (COE) = $C_{ann,tot}$ / E_{served}; where $C_{ann,tot}$ = total annualized cost of the system [€/yr] (based on the total net present cost of the system discounted at a 3.6%[6] real interest rate and 25 year lifetime) and E_{served} = total electrical load served (including grid sales) [kWh/yr]

[b] Calculated as NPC of Grid-only system (to meet same load as RE microgrid system) minus NPC of RE microgrid system; NPC = Sum of (Costs – Revenues) *$(1/(1+r)^n)$ where r = real interest rate (3.6%) and n = year of cash flow (out of 25 year project lifetime).

[6] Cost of capital is 5.6% for the Drink Water sector to borrow from the municipality, which is then adjusted by 2% for inflation, which is the average inflation rate from 1984-2013 (Trading Economics, 2014)

3. Results

This section explains the technical and economic potentials of various optimal system designs for grid connected and standalone systems. Abbreviations are used for the capacities of the system components, particularly in the graphs. For example, "GC_5.6MWpPV+4W+3MW/60MWhVRB+DR" refers to a grid-connected, 5.6MWp solar PV, 4 wind turbines (2MW each), 3MW cell stack – 60MWh electrolyte VRB flow battery storage combined with demand response. Similarly, "SA_2.8MWpPV+3W+1.3D+2MW/45MWhVRB+DR" refers to a stand-alone (not connected to grid), 2.8MWp solar PV, 3 wind turbines, 1.3MW diesel generator capacity (2x660kW), 2MW cell stack-45MWh electrolyte VRB flow batter storage with demand response system.

Figure 9 compares the annual solar PV production, wind power production, grid purchases, storage throughput and grid sales relative to normal onsite electricity demand (16.7 GWh/year) and how much total electricity demand can be served per year by excess RE production with flexible demand for grid-connected scenarios versus the current base case. Figure 10 provides a similar comparison between stand-alone microgrid configurations. Storage throughput and grid sales are graphically depicted as negatives since they are not consumed immediately but stored either onsite or in the main grid for later use.

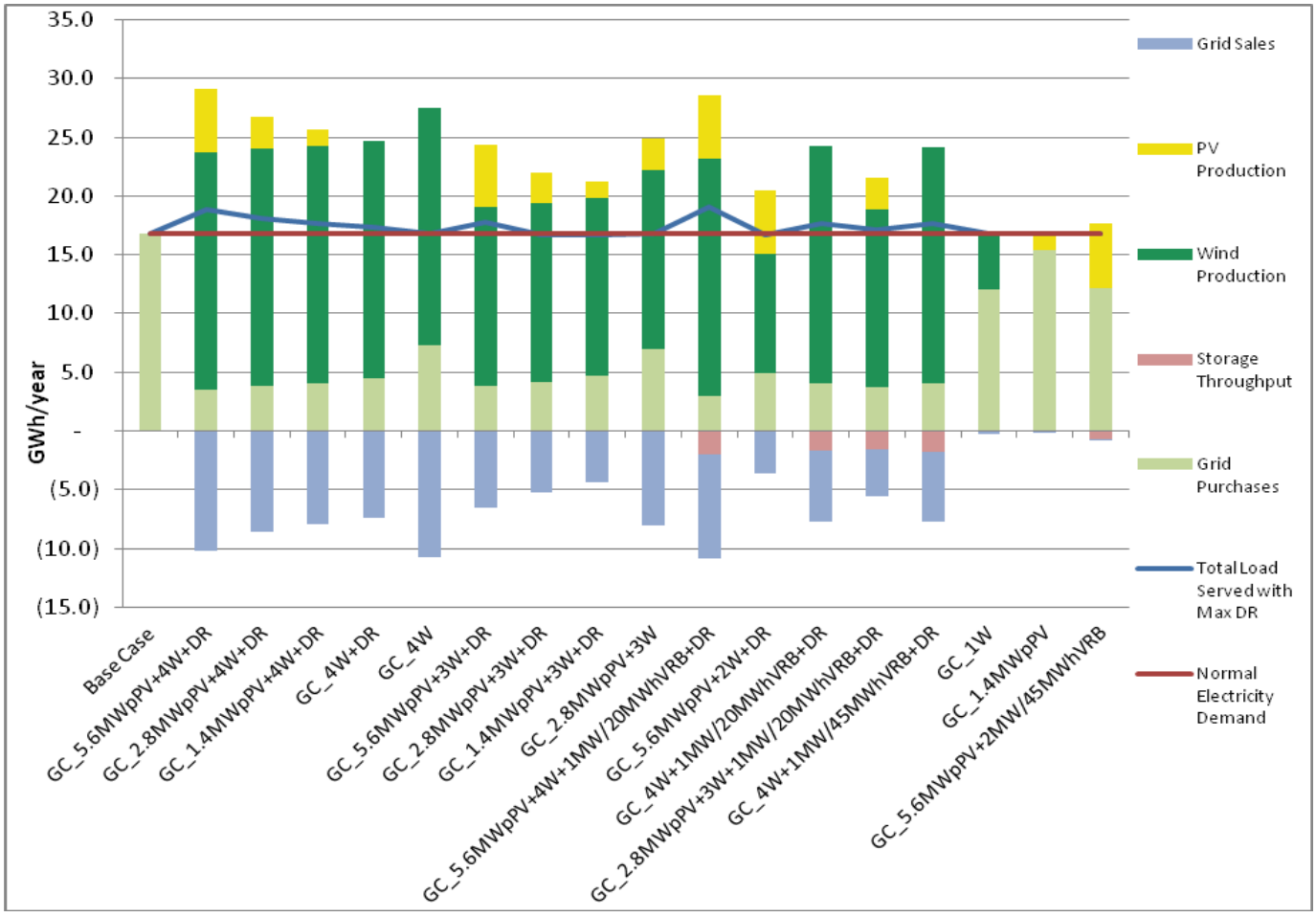

Figure 9. Annual PV and wind production, storage throughput and grid purchases relative to normal onsite electricity demand (16.7 GWh/year) for grid-connected scenarios (ordered by NPV from highest to lowest)

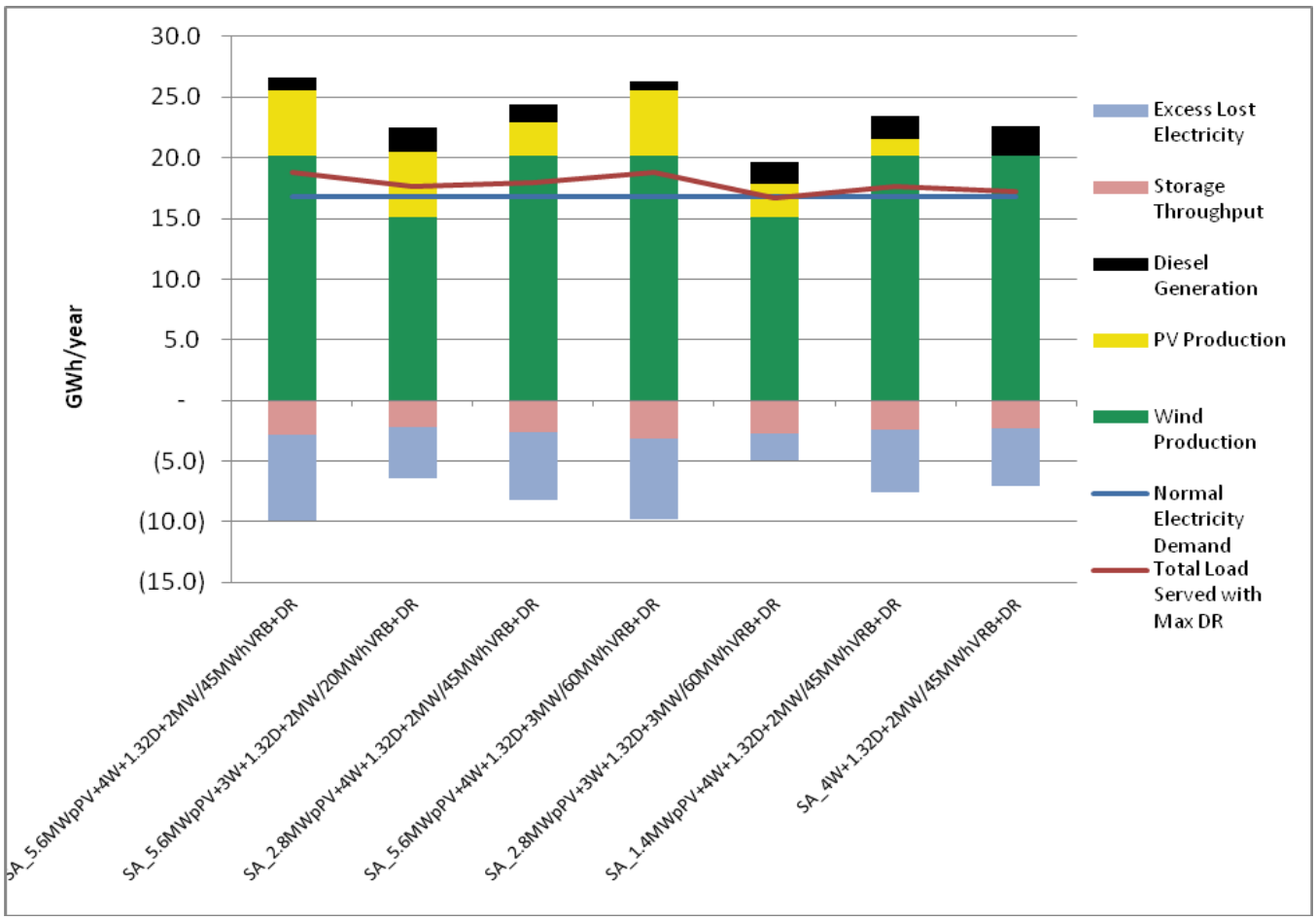

Figure 10. Annual PV and wind production, storage throughput, diesel power generation and excess lost electricity versus normal annual electricity demand (16.7 GWh/year) for stand-alone microgrid system configurations

A system configuration of maximum RE production capacity (5.6MWp solar PV[7] and 4 wind turbines of 8MW) combined with very large battery storage (3MW power/60MWh electrolyte VRB storage) and flexible demand (DR) can supply 96% of onsite electricity demand (stand-alone microgrid)[8]. In grid-connected scenarios, 90% of onsite power demand supplied by renewable electricity is possible with the same RE production capacity, yet a third of the storage capacity (1MW/20MWh VRB storage). This is just 2 percentage points higher than a system with the same RE capacity yet without the storage, which is still able to meet 88% of the onsite electricity demand.

These very high RE fractions are possible because the annual renewable electricity production potential is 25.6 GWh per year from 4 wind turbines (8MW) and 5.6 MWp Solar PV, which represent 79% and 21% of total renewable production, respectively. The maximum 25.6 GWh produced per year is 53% more electricity produced onsite than the normal 16.7 GWh annual power demand. Adding storage allows some of this excess renewable electricity to be

[7] Requires 36,000 m^2 of space if arrays can be arranged so that no additional space is needed between arrays to prevent them from casting shade on each other. If arrays need to be arranged with extra space in between them, this maximum solar PV capacity would require about twice as much space, and would therefore not entirely fit on Parcel Zuid.

[8] Even if storage capacity is doubled, the intermittency of wind and solar power does not permit 100% of load to be supplied by renewable electricity.

used at another point in time to meet the demand when production is low, causing the RE fraction of onsite demand to be 2-8% higher than systems without battery storage.

In grid-connected cases, the excess electricity, which is not stored, is exported back to the grid, which also increases the amount of renewable electricity on the main power grid network. Figure 9 illustrates that there are many grid-connected microgrid case configurations that produce significant amounts of excess electricity beyond onsite demand, which they sell back to the main grid, making the imported grid electricity more "green" in absolute terms. However, if there is no grid-connection, this excess renewable electricity is lost. In all stand-alone cases, the amount of excess electricity that is lost ranges from 2.2 GWh to 7.1 GWh, which can be even higher if maximum solar PV and wind capacities are implemented without battery storage. This is a problem in stand-alone microgrid scenarios since oversizing RE production makes them more cost-effective by minimizing the need for expensive diesel generation and storage, yet results in large losses of clean electricity.

Figure 11 illustrates the difference in levelized cost of electricity (COE) between the base case (red column) and the selected grid-connected (GC) and stand-alone (SA) microgrid systems (blue columns).

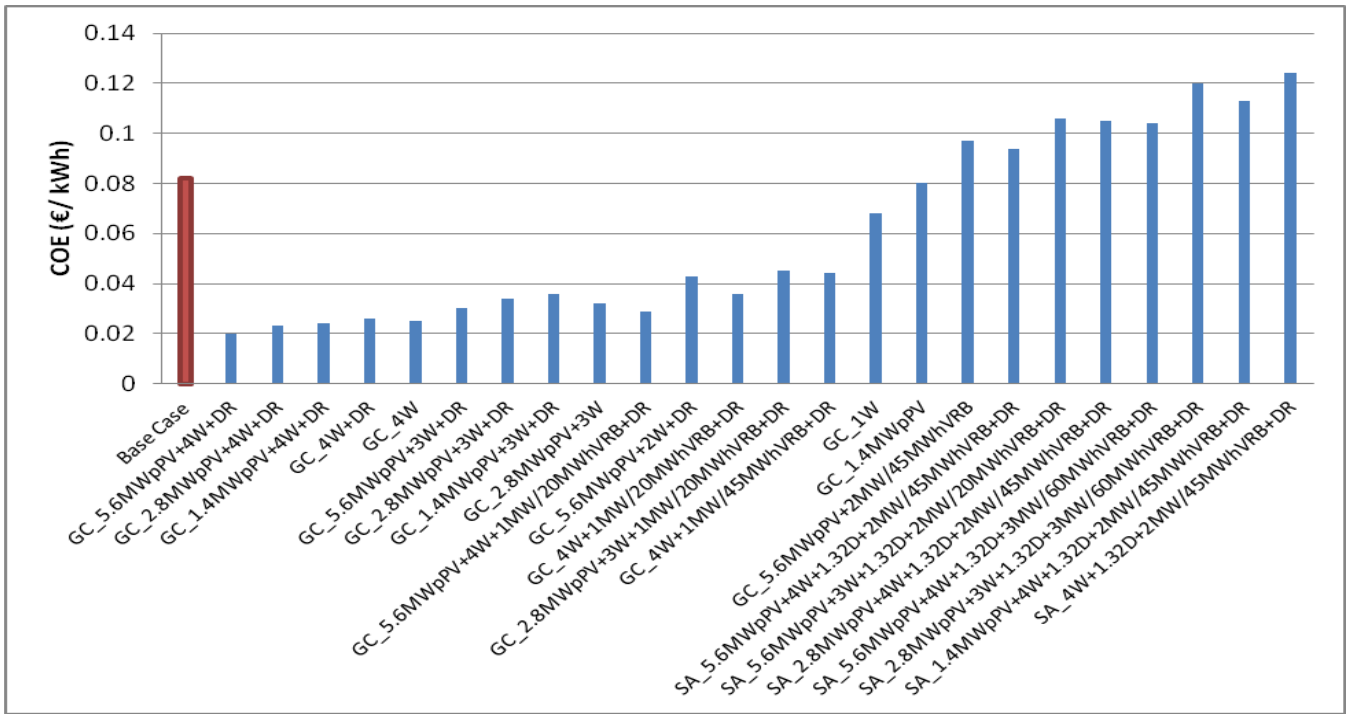

Figure 11. Summary comparing base case COE (red) to the chosen grid-connected and stand-alone system configurations

Grid-connected system configurations, containing 4 wind turbines (with or without solar PV) and without battery storage have the lowest cost of electricity (COE); between 0.020-0.026 €/kWh. This is 68% less than the current base case COE of 0.082 €/kWh since there is a significant drop in grid-imports due to onsite consumption and flexible demand.

System designs with 3 wind turbines combined with 2.8MWp or 5.6MWp Solar PV (without battery storage) have a COE between 0.030-0.036 €/kWh, which is 60% less than the current base case COE. This is also due to the onsite consumption and 5.2-6.5 GWh/year of grid sell-back. System configurations that do have VRB battery storage have a COE ranging from 0.036 – 0.097 €/kWh depending on the size of storage. Larger battery storage combined with

fewer wind turbines results in a higher COE since there is less excess low cost renewable electricity production that can be stored and used at a later time instead of importing from the grid.
Stand-alone system configurations have a minimum COE of 0.094 €/kWh for a 94% renewable design with maximum renewable production (5.6MWp Solar PV + 4 wind turbines) and the mid-sized battery storage option (2MW/45MWh VRB) with demand response. If storage is increased to the largest option (3MW/60MWh), the COE increases by 10 cents to 0.104 €/kWh since the high investment costs for the additional storage are still greater than the fuel cost saved by decreasing diesel generation by 27%. System designs without solar PV and only wind turbines have the highest COE, starting at 0.124 €/kWh or higher if the number of wind turbines in the system decreases causing the amount of diesel power generation to increase. Therefore, a solar-wind system combination is also optimal from a COE perspective since adding solar PV production minimizes the need for diesel generation.

Table 11 and 12 list the details of the different cases, including NPV and PBT, for grid-connected and stand-alone cases, respectively.

Table 11. Extracted system designs from overall optimization results for the current grid-connected models ordered by NPV (€million) (highlighted =with DR)

Microgrid System Design							Technical Potentials						2013 Economic Potentials		
DR	PV	V90	Gen (2)	Converter	VRB-ESS Battery Power	VRB-ESS Battery Storage	Total Annual RE Prod.	Total Ann. Load Served	Annual Grid Purch.	RE % of onsite load	Annual Grid Sales	Annual Battery Thruput	COE	NPV	Discounted PBP
Y/N	MWp	#	MW	MW	MW	MWh	GWh/yr	GWh/yr	GWh/yr	%	GWh/yr	GWh/yr	€/kWh	€ million	years
N	Base Case						-	16,7	16.7	0%	-	-	€0.082	-	0
Y	5.6	4	-	5.2	-	-	25.6	18.8	3.5	88%	10.2	-	€0.020	€12.7	7.2
Y	2.8	4	-	2.5	-	-	22.9	18.1	3.8	86%	8.6	-	€0.023	€12.4	6.1
Y	1.4	4	-	1.3	-	-	21.5	17.7	4.1	84%	7.9	-	€0.024	€12.2	5.6
Y	-	4	-	-	-	-	20.2	17.3	4.5	82%	7.4	-	€ 0.026	€11.8	5
N	-	4	-	-	-	-	20.2	16.7	7.3	74%	10.7	-	€0.025	€11.2	5.05
Y	5.6	3	-	5.2	-	-	20.5	17.7	3.9	84%	6.6	-	€0.030	€10.6	7.4
Y	2.8	3	-	2.5	-	-	17.8	16.7	4.2	81%	5.2	-	€0.034	€10.3	6.1
Y	1.4	3	-	1.3	-	-	16.5	16.7	4.7	78%	4.4	-	€ 0.036	€10.0	5.5
N	2.8	3	-	2.5	-	-	17.8	16.7	7.0	72%	8.0	-	€0.032	€9.6	6.4
Y	5.6	4	-	5.2	1	20	25.6	19.0	2.9	90%	8.8	2.4	€0.029	€9.3	10.9
Y	5.6	2	-	5.2	-	-	15.5	16.7	5.0	76%	3.6	-	€0.043	€8.2	7.8
Y	-	4	-	1.3	1	20	20.2	17.7	4.0	83%	6.1	1.7	€0.036	€8.2	9.5
Y	2.8	3	-	2.5	1	20	17.8	17.1	3.7	82%	4.0	1.6	€0.045	€6.9	11
Y	-	4	-	1.3	1	45	20.2	17.7	4.0	83%	6.0	1.8	€0.044	€5.2	15.4
N	-	1	-	-	-	-	5.0	16.7	12.0	30%	0.3	-	€ 0.068	€3.6	4.2
N	1.4	-	-	1.3	-	-	1.3	16.7	15.4	8%	0	-	€ 0.080	€0.6	12.6
N	5.6	-	-	5.2	2	45	5.6	16.7	12.1	31%	0.1	0.7	€0.097	€-5.0	n/a

Table 12. Extracted system designs from overall optimization results for the current stand-alone models ordered by NPV (€million) (all with DR)

Microgrid System Design							Technical Potentials						2013 Economic Potentials		
Grid	PV	Converter	V90	Gen (2)	VRB-ESS Battery Power	VRB-ESS Battery Storage	Total Annual RE Prod.	Annual Generator Prod.	Total Ann. Load Served	RE % of Load	Ann. Excess Elec-tricity	Annual Battery Throughput	COE	NPV	Discounted PBP
Y/N	MWp	MW	#	MW	MW	MWh	GWh/yr	GWh/yr	GWh/yr	%	GWh/yr	GWh/yr	€/kWh	€ million	years
N	5.6	5.2	4	1.32	2	45	25.6	1.1	18.8	94%	7.1	2.8	€0.094	€ -7.3	n/a
N	5.6	5.2	3	1.32	2	20	20.5	1.9	17.6	89%	4.2	2.2	€0.106	€ -7.7	n/a
N	2.8	2.5	4	1.32	2	45	22.9	1.5	17.6	91%	5.7	2.6	€0.105	€ -8.1	n/a
N	5.6	5.2	4	1.32	3	60	25.6	0.8	18.9	96%	6.6	3.2	€0.104	€ -9.3	n/a
N	2.8	2.5	3	1.32	3	60	17.8	1.8	16.7	89%	2.2	2.7	€0.120	€ -9.8	n/a
N	1.4	2.5	4	1.32	2	45	21.5	1.9	17.6	89%	5.1	2.5	€0.113	€ -9.8	n/a
N	-	2.5	4	1.32	2	45	20.2	2.4	17.2	86%	4.7	2.3	€0.124	€ -12.2	n/a

The results confirm that there is a high production potential for wind power and a relatively moderate production potential for solar PV power at this location in the middle of the Netherlands. With these significant combined potentials for renewable electricity production onsite, there are a multitude of system designs that can make the DWP greater than 70% self-sufficient from renewable electricity. Assuming that the space needed for the solar PV arrays has to be increased by a factor of 2 to prevent them for casting shade on each other and assuming the shadow cast by adding a 4th turbine would significantly influence the solar PV power production, the maximum fraction of onsite demand that can be met by renewable electricity ranges from 72-83% depending on the combined solar PV, wind, and battery capacity. In grid-connected microgrid cases, there are multiple microgrid configurations and sizes that can achieve this, which are cost-effective and even quite profitable. However, if the sizing assumptions and negative interactions can be avoided, up to 96% of the onsite power demand can be met by renewable electricity with maximum solar PV capacity (5.6MWp), maximum wind capacity (4 wind turbines of 8 MW), and large VRB flow battery storage of 3MW-60MWh combined with flexible demand (DR).

The results indicate even with these high RE production potentials, a 100% renewable system without grid imports or diesel generation would require significantly larger storage, which is already cost-ineffective, as seen in the non-profitable stand-alone cases. However, as long as there is grid-connection to sell back excess renewable electricity, microgrid configurations with moderately sized battery storage can still be cost-effective and profitable, although not necessary. The significantly higher wind potential for this area indicates that wind turbines should definitely be part of the energy mix. The solar PV potential is also substantial and creates a more balanced power supply onsite when combined with wind power. Therefore, a solar PV- wind turbine power production combination is optimal in this area and is the most cost-effective as long as there is grid-connection and sell-back to the grid.

4. Discussion of uncertainties

By modelling a variety of scenarios with different mixes of renewable component sizes, storage, diesel generation, and flexible demand (DR), the uncertainties around the technical potentials of meeting onsite demand with renewable electricity have been explored. However, due to the complexity of a microgrid and the multitude of integrated components, there are a number of major variables which are still uncertain and can influence the main economic potentials of this research (NPV & PBP).

It is found that if average electricity prices over the 25 year project period increase by 10%-30% from current prices, NPVs increase by 16%-55% and discounted PBP decreases by 8%-26%. This shows that the economic potentials are moderately to highly sensitive to changes in electricity prices and confirms that as electricity prices increase, investment in renewable energy technologies is more profitable and cost-effective since the avoided costs of using electricity from the grid are greater.

The discount rate is assumed to be the cost of capital, which is currently 5.6%. However, the method of financing, and in turn the cost of capital, is uncertain for such large projects at a public organization where renewable energy investments are not part of the core business. Figure 12 indicates that for every 2% change in discount rate, NPV changes by about 29% and discounted PBP changes by about 9%. This shows that economic potentials are highly sensitive to small changes in discount rate.

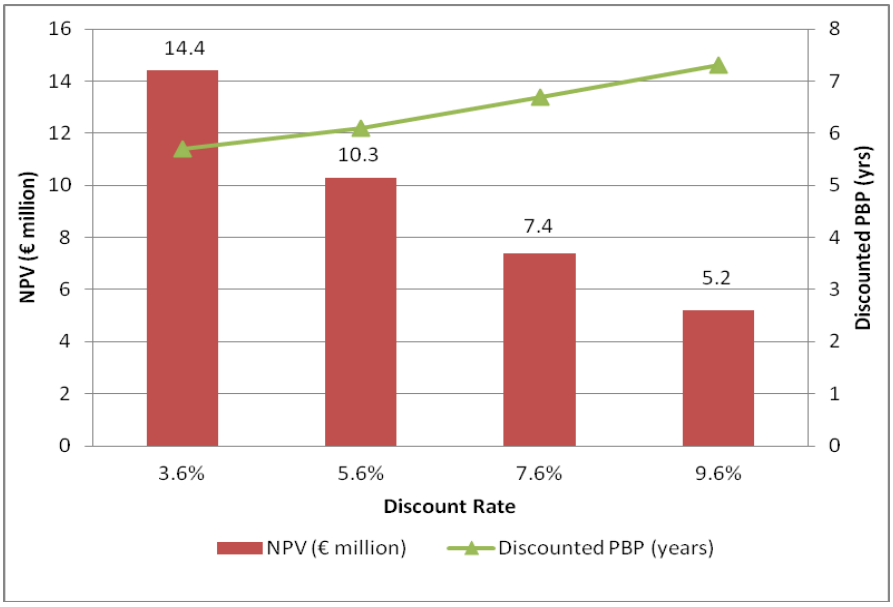

Figure 12. The effect of an increasing discount rate on NPV and discounted PBP for a 2.8MWp-3 wind turbine system configuration

Although lifetime assumptions were made based on manufacturer technical information, there is no guarantee that technologies will last as long as the manufacturer lifetimes. If all variable component lifetimes are 5 years shorter, NPVs decrease by 20%. If variable component lifetimes are 5 years longer, then NPVs increase by 13%. This slight sensitivity to different component lifetimes indicates that their effect on the economic potentials is small.

The costs calculations include tax incentives and subsidies[9]. Excluding these would decrease the NPVs by about 20% and increase the discounted PBPs by 50%.

This shows that the economic potentials are moderately sensitive to electricity price changes, and moderately to highly sensitive to changes in electricity prices and support schemes, and highly sensitive to changes in discount rates. However, overall in the worst or most extreme cases, the economic potentials remain acceptably cost-effective for grid-connected scenarios and not cost-effective for stand-alone scenarios.

The costs assumptions used for wind turbine, solar PV systems, and diesel generators were based on commercially available data as of the writing of this report. However, due to the novelty of VRB Flow batteries there is a wide range of costs since sizing and installation is site dependent so accurate cost data is not readily available. In order to mitigate this, the lower end of average costs were assumed in the range, which should be kept in mind when reviewing the techno-economic potentials of microgrid configurations that include battery storage. Similarly, the costs for demand response communication and control technology are not commercially available and are very case dependent depending on the needs of the site. However, relative to wind and PV costs, DR costs are not as significant and would not have a significant impact on the overall results.

[9] The EIA tax scheme leads to an advantage of 10% of the investment for PV and 4% for wind and the SDE+ subsidy to 1.5 mln EUR per wind mill and 162 EUR per kWp (based on Agentschap NL (2013a and b)).

Due to the inherently uncertain nature of modelling and the number of assumptions that need to be made, the validity and reliability of the model needs to be discussed.
Measured data wind speed, solar irradiation, and temperature for the exact location of the DWP was not available, which could cause discrepancies in the wind and solar power potential. However, measured data was used from a very nearby location (less than 15km away) with similar wind and solar characteristics to the DWP, which minimizes these discrepancies. Additionally, solar potential could be more accurate by using hourly measured solar irradiance rather than interpolating from monthly averages. It should also be kept in mind that these inputs and resulting potentials are case specific.
Furthermore, simplified assumptions were made about the flexibility of energy consumption based on the minimum pumping power and maximum pumping power of the pumps currently located at the DWP. Although this method is quite site specific based on the operating characteristics of the pumps on site, a minimum of 29% flexibility that is established can be assumed to be applicable in other industrial water treatment sites that distribute water since these also require either multiple pumps of increasing power ratings or large multi-frequency pumps that can function at different rating. However, this flexibility will also be dependent on specific consumer demands, network constraints, and storage capacities. For example, if the water transport network was more expansive so that the larger pumps could be used at this site, this would increase the flexibility of electricity consumption significantly since this would add another level of pumping. Linked to this, improvements could be made in the area of the prediction of water demand and weather conditions. The correlation between solar intensity and drinking water use on the one hand, and wind and rain on the other hand, might be used to optimize energy demand and supply.

5. Conclusions

The main aim of this research was to explore the techno-economic potential for a predominantly renewable electricity-based microgrid serving an industrial-sized drink water plant in the Netherlands since there have been no documented cases or research done for a microgrid serving this type of electricity demand in the Dutch context. Therefore, grid-connected and stand-alone microgrid scenarios were modelled using Waternet's drink water treatment plant in Nieuwegein as a case study.

Utilizing measured wind speed and solar irradiation data from a nearby town, real time manufacturer data for technology components, and a bottom-up approach to model a flexible demand from demand response, the modelled results show that **t**here is a very high potential for renewable electricity at the site, which can make this drink water treatment plant's electricity consumption between 70-96% self-sufficient with renewable electricity from solar PV and wind power production. Wind production potential is very high onsite and can meet 82% of onsite demand without adding solar PV. However, PV production potential is also substantial and provides a more balanced supply which can supply electricity at times when wind production is insufficient. Due to the supplemental supply over different parts of the day, adding solar PV also increases the benefits gained from the demand response strategy. Therefore, a solar-wind system combination is recommended over a wind only system.

It is found that grid-connected microgrid systems which can sell excess electricity beyond the demand, have positive NPVs. The most profitable system configuration is a 5.6MWp Solar PV – 8MW wind (4 turbines) combined with demand response, yet without storage. The microgrid system can be 88% self-sufficient on renewable electricity, with a COE of 0.020 €/kWh, an NPV of €12.7 million, and a payback period of 7.3 years. If this system is combined with large storage, the 25.6 GWh/year of locally produced renewable electricity can supply up to 96% of the onsite electricity demand. However, due to the large storage capacity which is still very expensive, and even has a negative NPV in stand-alone systems since 6.6 GWh/year of excess electricity is lost instead of sold-back to the grid and diesel fuel costs are high. The least cost stand-alone system can meet 94% of onsite demand with maximum RE capacities with slightly smaller but still large battery storage, yet it has a COE of 0.94 €/kWh, which is 12 cents more expensive than currently buying all electricity from the grid. Although these stand-alone cases prove that an industrial-sized water treatment plant can continue operating without grid-connection, it is not profitable for an industrial electricity load to be completely independent from the grid in the Netherlands when it can receive very low wholesale electricity prices. Therefore in the case of the DWP, disconnecting from the main grid should only be done in emergency situations.

Relative to other industries, which may require significantly more heat for the production process, the drink water treatment industry is special in that it has a relatively low thermal demand. Therefore, the resulting predominantly RE based microgrid from this research is particularly suitable for the drink water industry and not necessarily applicable to other industrial process sites which have a different mix of energy demand. Nonetheless, onsite self-sufficiency with a microgrid system could still be an option for other types of industrial sites, but would require different components like cogeneration (CHP) technology as part of the microgrid energy mix in order to more efficiently meet heat demand. Depending on the land and resources available, this could still be renewable if fuelled with biomass. Ultimately, becoming self-sufficient via a microgrid system is relevant to many industries, but the energy mix and system configuration is very much case dependent.

References

Agentschap (2013a). Energie-investeringsaftrek (EIA): energielijst 2013. Retrieved on 4 april 2013 from: http://www.rvo.nl/sites/default/files/Energie%20investeringsaftrek%20-%20Energielijst%202013_1.pdf

Agentschap (2013b). SDE+ 2013: Zo vraagt u subsidie aan voor de productie van duurzame energie. Retrieved on 14 March 2013 from Agentschap NL Ministerie van Economische Zaken: http://www.agentschapnl.nl/sites/default/files/Printversie%20digitale%20brochure%20SDE+%202013.pdf

Andrews, J. and Jelley, N. (2007). Energy Science: Principles, technologies, and impacts. Oxford University Press.

Boer, P. And Raadschelders, J. (2007). Briefing Paper: Flow Batteries. KEMA, Netherlands. Retrieved on 18 April 2013 from Leonardo Energy: http://www.leonardo-energy.org/sites/leonardo-energy/files/root/pdf/2007/Briefing%20paper%20-%20Flow%20batteries.pdf

Braam, Hein (2013). *Procesvoerder- Regelcentrumat at Waternet.* Interviewed on 7 March 2013 [additional email follow-ups on 12 & 14 March 2013, 6 May 2013]

Budikova, D., Hogan, M., Hall-Beyer, M., Hassan, G., Pidwirny, M. (2012). Albedo. Encyclopedia of Earth. Eds. Cutler J. Cleveland. Washington, D.C.: Environmental Information Coalition, National Council for Science and the Environment, USA. Retrieved March 28, 2013 from http://www.eoearth.org/article/Albedo?topic=54300

Cobben, J.F.G. (2008) More Microgrids Project: The first microgrid in the Netherlands Retrieved on December 27, 2012 from: http://der.lbl.gov/sites/der.lbl.gov/files/Cobben_2008.pdf

Community for Energy, Environment, & Development (COMMEND) (2012). Modelling Software. Retrieved on 24 February 2013 from: http://www.energycommunity.org/default.asp?action=71

Connelly, D., Lund, H., Mathiesen, B.V., Leahy, M. (2010). A review of computer tools for analysing the integration of renewable energy into various energy systems. Applied Energy 87. Pp. 1059-1082.

CSUN (2012). QSAR 260 Series. Retrieved on 28 March 2013 from China Sunergy: http://www.chinasunergy.com/en/product/81

Diesel Service & Supply (2013). Approximate Diesel Fuel Consumption Chart. Retrieved on 16 April 2013 from : http://www.dieselserviceandsupply.com/Diesel_Fuel_Consumption.aspx

Dohn, L. R. (2011). The business case for microgrids White paper: The new face of energy modernization, s.l.: Siemens AG.

Duffie, J.A. and Beckman, W.A. (1991) .Solar Engineering of Thermal Processes 2nd edition, Wiley, New York, NY

Electricity Storage Association (ESA) (2011). Technology Comparison. Retrieved on 18 April 2013 from: http://www.electricitystorage.org/technology/storage_technologies/technology_comparison

GeneratorJoe (2013). Products. Retrieved on 23 April 2013 from: http://www.generatorjoe.net/price.asp?30=75001+and+100000

Guerrero, J.M. (2010). Microgrids: Integration of distributed energy resources into the smart-grid, Industrial Electronics (ISIE), 2010 IEEE International Symposium on , vol., no., pp.4281,4414, 4-7 July 2010

Guerrero, J. M. (2013). What are microgrids? IEEE Industrial Electronics Magazine, 2013, vol. 4.

Haberlin, H. (2012). Photovoltaics: System Design and Practice. A John Wiley & Sons, Ltd.,

Publication.
Heck, G. (2013). *Assetmanager – Assetmanagement en Beleid at Waternet*. Interviewed on 5 May 2013 [additional email follow-ups on 7 & 8 May 2013]
HOMER Energy (2013). Optimizing Clean Power Everywhere: Energy Modelling Software for Hybrid Renewable Energy Systems. Retrieved on 24 February 2013 from HOMER Energy: http://www.homerenergy.com/
Irie, H. (2012). Sendai Microgrid - Introduction and Use Case. Retrieved on January 11, 2013 from: http://e2rg.com/microgrid-2012/Sendai_Irie.pdf
EPRI (2003). Costs of Utility Distributed Generators, 1-10MW: 24 Case Studies. Palo Alto, CA and Cooperative Research Network, Arlington, VA: March 2003. Technical Update 1007760.
Knibbe, Adriaan (2013). 130227 Elektriciteitskosten WCB Groenendael. Internal electricity cost budget calculations Waternet, Amsterdam.
KNMI (2012). KNMI Weer Dataset 2012. Retrieved on 20 March 2013 from Royal Netherlands Meteorological Institute: https://data.knmi.nl/portal-webapp/KNMIDatacentrum.htmlKors, Leon (2013). *Teamleider - Waterkwaliteit en Procesonderst at Waternet*. Interview during plant tour on 1 March 2013.
Lambert, T. (2007). How HOMER Calculates the PV Array Power. Output. Homer Help File, 2007. http://homerenergy.com/.
Lambrechts, H. (2012). PV-Installatie Zonneweide Leiduin. Internal Waternet EPC – contract with Sunproject NV.
Lantz, E., Wiser, R., & Hand, M., (2012). IEA Wind Task 26: The Past and Future Cost of Wind Energy. National Renewable Energy Laboratory. Technical Report. Pp. 18-27.
Lenntech (2012). A drinking water purification process. Retrieved on 2 April 2013 from Lenntech BV: http://www.lenntech.com/applications/drinking/purification/drinking-water-preparation.htm
Lindemann, J.H. (2004). Wind and solar powered seawater desalination: Applied solutions for the Meditteranean, the Middle East and the Gulf Countries. Desalination 168. Pp. 73-80.
Mahmoudi, H., Abdul-Wahab, S.A., Goosen, M.F.A., Sablani, S.S., Perret, J., Ouagued, A., Spahis, N. (2008). Weather data and analysis of hybrid photovoltaic-power generation systems adapted to a seawater greenhouse desalination unit designed for arid coastal countries. Desalination 222. Pp. 119-127.
Manwell, J.F., McGowan, J.G., and Rogers, A.L. (2009) Wind Energy Explained: Theory, Design and Application. 2nd edition. John Wiley and Sons, Ltd.
Meer, G.R.v.d. (2012). Inventarisatie zon PV Waternet: Haalbaarheid op basis van verschillen in elektriciteitprijs. Internal Waternet Publication. 8 November 2012.
Meer, Gijs (2013). *Adviseur - Werktuigbouw en Procestechniek at Waternet.* Interviewed on 10-11 April 2013 [with additional email correspondence]
Prudent Energy VRB System (2012). VRB Energy Storage Systems. Retrieved on 22 April 2013 from: http://pdenergy.com/vrb-energy-storage-systems.php
Ramos, J.S. & Ramos, H.M. (2009). Sustainable application of renewable sources in water pumping systems: Optimized energy system configuration. Energy Policy 37. Pp 633-643.
Renewable Energy Concepts (2012). Solar Basics. Retrieved on 27 March 2013 from: http://www.renewable-energy-concepts.com/solarenergy/solar-basics/tilt-angle-pv-array.html

Ritzen, A. & Gastel, V. (2012). Quick Scan Windenergie: 13 locaties voor Waternet. Study done by Ecorys Consulting on behalf of Waternet B.V. 20 May, 2012.

Stouten, B. & Pinksteren, J.A.W. van (2010). Voorontwerp Pilot Beveiliging Transportnet WCB. Waternet Onderzoek & Projecten Report. Waternet, Amsterdam.

Sungrow (2013). Company Profile. Retrieved on 28 March 2013 from Sungrow Power Supply Co., Ltd: http://www.sungrowpower.com/sungrow-english/about.php?page=1

Trading Economics (2014). Inflation rates for the Netherlands. Accessed 5 January 2014. http://www.tradingeconomics.com/netherlands/inflation-cpi

Urmee, T., Harries, D., & Schlapfer, A., (2009) Issues related to rural electrification using renewable energy in developing countries of Asia and Pacific. Renewable Energy, 34 (2). pp. 354-357

Velden, B.S.v.d. (2011). Waternet-Meest rendabele functie van een parceel op basis van kosten-batenanalyse. Thesis for Hogeschool van Hall Larenstein. Vastgoed en grondtransacties opleiding.

Vestas (2012). 2 MW: V80-2.0 MW, V90-1.8/2.0 MW, V100-1.8/2.0 MW. Retrieved on 20 March, 2013 from Vestas Wind Systems A/S: http://nozebra.ipapercms.dk/Vestas/Communication/Productbrochure/2MWTurbineBrochure/2MWMrk7US

WateReuse (2011). Seawater Desalination Power Consumption. Watereuse Association Desalination Committee. White Paper. November 2011. Retrieved on 25 February 2013 from: http://www.watereuse.org/sites/default/files/u8/Power_consumption_white_paper.pdf

Waternet (2012a). KPI KWh per m3 2012 vereenvoudigd. Internal production calculation Waternet, Amsterdam.

Waternet (2012b). FROM SEEPAGE WATER TO TAP WATER in 12 steps. Brochure produced by Waternet.

Waternet (2013a). Energie WCB, Groenendael 6. Internal energy use file. Waternet, Amsterdam.

Waternet (2013b). Energie per Process, Groenendael 6. Internal electricity use calculation. Waternet, Amsterdam.

Waternet (2013c). Proces info Nieuwegein: Pumps WRK. Internal information and process file. Waternet, Amsterdam.

Wind Energy, The Facts (2009). Cost of on-land wind power: Investment Costs. Retrieved on 21 March, 2013 from Wind Energy, The Facts: http://www.wind-energy-the-facts.org/en/part-3-economics-of-wind-power/chapter-1-cost-of-on-land-wind-power/cost-and-investment-structures/

WWI (2012). Operational and Maintenance Costs for Wind Turbines. Retrieved on 21 March, 2013 from Wind Measurement International: http://www.windmeasurementinternational.com/wind-turbines/om-turbines.php